JOURNAL OF VIROLOGY, Dec. 1995, p. 7724–7733 Vol. 69, No. 12
0022-538X/95/$04.00+0


# Branchpoint and Polypyrimidine Tract Mutations Mediating the Loss and Partial Recovery of the Moloney Murine Sarcoma Virus MuSVts110 Thermosensitive Splicing Phenotype

JEFFREY W. TOUCHMAN,[1] IAN D'SOUZA,[2] CAROLINE A. HECKMAN,[2] RONG ZHOU,[2] NEAL W. BIGGART,[3] AND EDWIN C. MURPHY, JR.[2]*

*Molecular Virology Section, Department of Tumor Biology, University of Texas M.D. Anderson Cancer Center, Houston, Texas 77030[2]; National Center for Human Genome Research, National Institutes of Health, Bethesda, Maryland 20892[1]; and Department of Biology, San Diego State University, San Diego California 92182-0057[3]*

Received 8 November 1994/Accepted 11 September 1995

**Balanced splicing of retroviral RNAs is mediated by weak signals at the 3′ splice site (ss) acting in concert with other *cis* elements. Moloney murine sarcoma virus MuSVts110 shows a similar balance between unspliced and spliced RNAs, differing only in that the splicing of its RNA is, in addition, growth temperature sensitive. We have generated *N*-nitroso-*N*-methylurea (NMU)-treated MuSVts110 revertants in which splicing was virtually complete at all temperatures and have investigated the molecular basis of this reversion on the assumption that the findings would reveal *cis*-acting elements controlling MuSVts110 splicing thermosensitivity. In a representative revertant (NMU-20), we found that complete splicing was conferred by a G-to-A substitution generating a consensus branchpoint (BP) signal (-CCCUGGC- to -CCCUGAC- [termed G(−25)A]) at −25 relative to the 3′ ss. Weakening this BP to -CCCCGAC- [G(−25)A,U(−27)C] moderately reduced splicing at the permissive temperature and sharply inhibited splicing at the originally nonpermissive temperature, arguing that MuSVts110 splicing thermosensitivity depends on a suboptimal BP-U2 small nuclear RNA interaction. This conclusion was supported by results indicating that lengthening the short MuSVts110 polypyrimidine tract and altering its uridine content doubled splicing efficiency at permissive temperatures and nearly abrogated splicing thermosensitivity. In vitro splicing experiments showed that MuSVts110 G(−25)A RNA intermediates were far more efficiently ligated than RNAs carrying the wild-type BP, the G(−25)A,U(−27)C BP, or the extended polypyrimidine tract. The efficiency of ligation in vitro roughly paralleled splicing efficiency in vivo [G(−25)A BP > extended polypyrimidine tract > G(−25)A,U(−27)C BP > wild-type BP]. These results suggest that MuSVts110 RNA splicing is balanced by *cis* elements similar to those operating in other retroviruses and, in addition, that its splicing thermosensitivity is a response to the presence of multiple suboptimal splicing signals.**

During RNA splicing, the identification-juxtaposition of splice sites (ss) and the catalysis of splicing reactions are mediated by RNA-RNA and RNA-protein interactions between the pre-mRNA and components of the splicing machinery. Initially, a commitment complex is formed in which the 5′ ss is specified by base pairing with U1 small nuclear RNA (snRNA), which, acting in concert with SR proteins, contributes to the binding of U2AF to the polypyrimidine tract adjacent to the 3′ ss (10, 50, 51, 60, 65, 69). After the commitment phase, the branchpoint (BP) sequence, which is usually located 18 to 40 nucleotides upstream of the 3′ ss, is recognized by base pairing with U2 snRNA, this interaction being stabilized by U2AF already recruited to the polypyrimidine tract (29, 66). Hence, the stability of the BP-U2 snRNA interaction depends on the mutual complementarity of the BP and U2 snRNA as well as the affinity of the polypyrimidine tract for U2AF, an affinity which is influenced by the length, position, and pyrimidine content of the tract (14, 16, 34, 43, 45). After 5′ ss recognition, U1 snRNA appears to be dispensable and is displaced by U6 snRNA (25, 28, 30, 62), which interacts with at least two nucleotides in the 5′ ss (47, 48, 54, 62) and, at the same time, forms intermolecular helices with the U2 snRNA paired with the BP. In the first splicing reaction, the 5′ ss, possibly held in position by U6-U2 snRNA helix III (59), is attacked by the BP adenosine, yielding two products: free exon 1 and lariat-exon 2. The efficiency of this reaction is influenced by the strength of several pre-mRNA–spliceosome component interactions, prominent among which is the complementarity between the BP sequence and U2 snRNA (63, 68, 69). In the second splicing reaction, the hydroxyl group at the 3′ end of exon 1 attacks the 3′ ss (which the polypyrimidine tract may help to select by a scanning mechanism [52, 53]), thereby ligating the exons and liberating the intron as a lariat. A conserved loop in U5 snRNA which interacts with exon sequences immediately adjacent to the 5′ and 3′ ss (37, 38, 54, 64) may help align the exons for the second splicing reaction (54).

For successful replication, the primary retroviral transcript encoding the replicative genes (*gag*, *pol*, and *env*) must undergo a special case of alternative splicing. Approximately 30 to 50% of this transcript is spliced to yield the *env* gene mRNA; the remainder escapes splicing and is transported to the cytoplasm, in which some serves as mRNA for the *gag* and *pol* gene products and some is packaged as the virion genetic material. There is substantial documentation that the avoidance of the splicing pathway by retroviral pre-mRNA is mediated by suboptimal splicing signals at the 3′ ss acting in concert with other positive and negative *cis*-regulatory elements (1a, 2, 15, 19, 24, 26, 27, 33, 57, 58). In avian sarcoma viruses (ASV), for example, a suboptimal BP signal is critical for the maintenance of

* Corresponding author.

the proper balance between unspliced *gag-pol* and spliced *env* RNAs. Insertion of an oligonucleotide linker near the *env* gene 3′ ss caused excess production of spliced *env* RNA and a concomitant replication defect. Oversplicing was determined to be a consequence of the introduction of two near-consensus BPs which relieved a block to wild-type (wt) splicing normally occurring prior to the first splicing reaction (15, 26, 27). The oversplicing phenotype could be suppressed by a mutation within the linker-inserted BP consensus sequence, resulting in a blockade of the second splicing reaction (15). Recently, it has been shown that this second-step block could be relieved and then restored by manipulation of the length and uridine content of the polypyrimidine tract at the *env* 3′ ss (7). In addition to ASV, the contribution of suboptimal *cis* signals in the BP and polypyrimidine tract to the regulation of splicing has been reported for Rous sarcoma virus, in which a suboptimal *env* 3′ ss acts in concert with a negative regulator in the intron to limit *env* mRNA splicing (32) and in which a suboptimal polypyrimidine tract helps to limit the amount of spliced *src* RNA produced (67), and also for human immunodeficiency virus type 1 (HIV-1), in which mutations generating a globin gene BP signal near the *tat*/*rev* 3′ splice site produce a large increase in splicing efficiency (55).

Moloney murine sarcoma virus MuSVts110 has been shown to adhere to the general retroviral RNA splicing strategy, differing only in that the splicing of its RNA, in addition to being balanced, is growth temperature sensitive. At 33°C and less, 30 to 50% of MuSVts110 transcripts are spliced such that the *gag* and *mos* coding sequences are placed in register, allowing the translation of $p85^{gag\text{-}mos}$ and, as a consequence, cell transformation. However, at temperatures above 37°C, MuSVts110 RNA is negligibly spliced (9). Consequently, MuSVts110-infected cells remain morphologically normal at physiological temperatures and above (21, 23, 35, 36). Our previous studies have shown that MuSVts110 RNA splicing is *cis* regulated in part by the strength of the BP, since introduction of a β-globin BP into a splicing-negative mutant of MuSVts110 activated splicing that was both very efficient and temperature insensitive (11), and also by a negative regulator in the second exon (the exon 2 distal element [E2DE]) (12, 56). Removal of the E2DE relaxes the interference with splicing observed at higher growth temperatures without producing a pronounced enhancement of splicing at the lower temperatures (56). From these results, it was inferred that the E2DE selectively interfered with splicing at higher temperatures, whereas the BP signals was more directly involved in the determination of splicing efficiency, and, if sufficiently strong, could override the dampening effect of the E2DE at high growth temperatures.

In this study, we found that conversion of the balanced, thermosensitive splicing phenotype in MuSVts110 to one much more like those of other cellular pre-mRNAs, in which "all or none" splicing is common, could be accomplished by a point mutation generating a consensus BP sequence near the MuSVts110 3′ ss and that much of the original splicing thermosensitivity could be recovered by lessening the complementarity of this BP with U2 snRNA. Moreover, increasing both the overall length of the wt MuSVts110 polypyrimidine tract and extending uridine stretches embedded in the tract had effects on splicing that were very similar to but not quite as pronounced as those of provision of a consensus BP. These observations suggested that MuSVts110 RNA splicing is balanced by *cis* elements at the 3′ ss similar to those operating in other simple retroviruses and, in addition, that its splicing thermosensitivity is an unusual response to the presence of multiple suboptimal splicing signals.

## MATERIALS AND METHODS

**Cell cultures and DNA transfection.** NRK cells infected with MuSVts110 (6m2 cells) (6) were maintained at 33°C in McCoy medium containing 10% bovine serum supplemented with transferrin (Hyclone). Revertants of the 6m2 line arising either spontaneously or induced by treatment with *N*-nitroso-*N*-methylurea (NMU) were maintained at either 37 or 39°C in the same medium. NIH 3T3 cells were maintained in Dulbecco high-glucose medium containing 10% bovine serum. Transfected NIH 3T3 cell lines were established in Dulbecco high-glucose medium containing 10% fetal bovine serum and were then transferred to the same medium containing 10% bovine serum (Hyclone). DNA transfection was carried out by a standard calcium phosphate coprecipitation protocol (20) with linearized viral DNA and pSV2neo DNA. G-418-resistant cells were selected in medium containing 400 μg of G-418 (Geneticin; Life Technologies) per ml.

**NMU mutagenesis.** 6m2 cells were treated with NMU and revertants were selected as described previously (3, 4). Briefly, 6m2 cells growing at 33°C were treated with 0.001 to 1 mM NMU for 24 h and then shifted to 39°C. Revertants growing as transformed foci at 39°C were picked after about 2 weeks. Cells from these revertant foci were then reselected after growth in soft agar at 39°C and grown in bulk.

**Cellular DNA isolation and PCR amplification.** Genomic DNAs from 6m2 and NMU revertant cells were isolated after cell lysis in 2% sodium dodecyl sulfate (SDS)–7 M urea–0.35 M NaCl–1 mM EDTA–20 mM Tris (pH 8.0), hybridized to a variety of MuSVts110-specific primer pairs depending on the experiment, and amplified with *Taq*I DNA polymerase as described previously (3, 8). The primer pairs used to amplify MuSVts110 DNA in NMU-20 cells were as follows. The SUZ1-SUZ4 pair (31) amplified MuSVts110 nucleotides 1972 to 2972, covering the 5′ end of E1, the 431-nucleotide intron, and 496 nucleotides of E2. SUZ1 (5′-CCCACTCAACTGCCCAATGAAGTCGA-3′) is complementary to MuSVts110 nucleotides 1970 to 1995, while SUZ4 (5′-TAGATGACTTG GTGTAGAGTCACGT-3′) is complementary to nucleotides 2973 to 2948. The SUZ3-RZ3 pair amplified MuSVts110 nucleotides 2520 to 3825, covering the rest of E2 and extending 41 nucleotides into the U3 region. SUZ3 (5′-TCTAA GCCTGTGTCGCTACCTCCCT-3′) is identical to the MuSVts110 plus strand at nucleotides 2520 to 2544, while RZ3 (5′-ACTTAAGCTAGCTTGCCACCT ACG-3′) is complementary to nucleotides 3825 to 3802. PCR-amplified DNA fragments were analyzed in 2% Nu-Sieve (FMC Colloids) gels in E buffer (40 mM Tris [pH 7.5], 5 mM NaOAc, 1 mM EDTA) or in 5% polyacrylamide gels in TBE buffer (90 mM Tris [pH 7.9], 90 mM boric acid, 3 mM EDTA).

**Single-strand conformational polymorphism (SSCP) analysis (39, 40).** To screen for NMU-induced mutations, cellular DNA from NMU-20 or control 6m2 cells was also amplified by using the following sets of MuSVts110-specific primer pairs. The JT5-CH2 pair amplified MuSVts110 nucleotides 2377 to 2535. JT5 (5′-CCCGGAAGAAAGAGAGGAAC-3′) is complementary to the MuSVts110 minus strand at nucleotides 2377 to 2396, and CH2 (5′-GCGACACAGGCT TAGAGGCG-3′) is complementary to the plus strand at nucleotides 2516 to 2535. The JT5-JEFF1 pair amplified MuSVts110 nucleotides 2377 to 2578. JEFF1 (5′-AGGACCGCGAGTCTACCG-3′) is complementary to the plus strand at nucleotides 2561 to 2578. The JT6-CH1 pair amplified MuSVts110 nucleotides 2327 to 2504. JT6 (5′-CTTGGAGATTTGGTTAGAGA-3′) is complementary to the minus strand at nucleotides 2327 to 2347, and CH1 (5′-CCT CAGATGGGACAGTCACA-3′) is complementary to the plus strand at nucleotides 2484 to 2504. After amplification, an equal volume of gel loading dye (98% formamide, 20 mM NaOH, 10 mM EDTA, 0.05% bromophenol blue, 0.05% xylene cyanol) was added to the DNA, following which it was denatured by being heated at 95°C for 5 min and quickly chilled on ice. The denatured DNA was immediately loaded onto a 9% polyacrylamide gel containing 5% glycerol, and the gel was run overnight at 200 V in 0.5× TBE while the temperature was maintained at 20°C. After electrophoresis, the gel was silver stained (Bio-Rad, Hercules, Calif.).

**DNA sequencing.** For sequencing, PCR products were enriched for the positive strand by amplification with only upstream primers (either SUZ1 or SUZ3, depending on which product was to be amplified). This product was then directly sequenced with internal primers (39, 40). Sequencing was carried out with the Sequenase primer extension kit (U.S. Biochemicals) as recommended by the supplier, except that the extension step was performed at 50°C. In some experiments, the double-stranded PCR product was sequenced directly with the same primers.

**Construction of viral mutants. (i) BP mutants.** To generate the MuSVts110 mutant containing a G-to-A substitution at nucleotide 2452 [termed MuSVts110: G(−25A)] NMU-20 cellular DNA was amplified with the SUZ1-JEFF1 primer pair in a PCR mixture containing 1 μg of NMU-20 genomic DNA, 1 μM each primer, 200 μM deoxynucleoside triphosphates, 1× reaction buffer (Perkin-Elmer), and 2.5 U of *Taq*I DNA polymerase (Perkin-Elmer). The product was digested with *Xho*I-*Acc*I and inserted into *Xho*I-*Acc*I-digested wild-type MuSVts110 DNA. To generate a MuSVts110 mutant containing both the G-to-A substitution at nucleotide 2452 and a T-to-C substitution at position 2450, viral DNA containing the G(−25)A mutation was used as a template for PCR-mediated directed mutagenesis. A primer pair, in this case the mutant primer JT17 (5′-CCC**C**GACTGTTCCTAATCATT-3′, complementary to nucleotides 2447 to 2467 with a mismatch [underlined in boldface] at nucleotide 2450) and

JT18 (5′-AGTTTGGGAGCATGG-3′), complementary to nucleotides 2445 to 2431), was selected such that their 5′ ends were juxtaposed. The JT17 primer introduced the T-to-C substitution into the PCR product. Amplification proceeded in opposite directions around the plasmid, resulting in a PCR product the size of linear pBB:G(−25)A. The PCR product was purified, phosphorylated, and circularized with T4 DNA ligase, resulting in the double substitution mutant pBB:U(−27)C. The *Xho*I-*Acc*I fragment of pBB:U(−27)C was then cloned into the MuSVts110 DNA digested with *Xho*I-*Acc*I to create the U(−27)C mutant.

**(ii) Polypyrimidine tract mutants.** To generate the MuSVts110 polypyrimidine tract mutant containing A-to-T nucleotide substitutions at nucleotides 2461, 2462, and 2465, a primer pair, in this case wt JT9 (5′ CAGCCAGGGAAGTTT GGGAG 3′, complementary to nucleotides 2455 to 2436) and mutant JT8a (5′ TTCCT**TT**TC**T**TTTCTCCCTAGTGTCTCATGTG 3′, complementary to nucleotides 2457 to 2487) was selected such that their 5′ ends were juxtaposed. Amplification yielded a product the size of linear pBB which was purified, phosphorylated, and circularized with T4 DNA ligase. The resulting triple mutant, pBB:19Y-4U (19 pyrimidines containing 4 consecutive uridine residues), was digested with *Xho*I-*Acc*I and introduced into similarly digested wt MuSVts110 DNA. In the second MuSVts110 polypyrimidine tract mutant, a further C-to-T mutation was introduced at nucleotide 2464. In this case, by a strategy identical to the one described above, pBB:19Y-4U DNA was amplified with the wt JT9 and JT8C mutant primer (5′TTCCTTTTTTTTTCTCCCTAGTGTCTC ATGTG 3′, complementary to nucleotides 2457 to 2487). Amplification and cloning yielded the quadruple mutant pBB/19Y-9U, whose *Xho*I-*Acc*I fragment was subcloned into wt MuSVts110.

**Cell labeling and immunoprecipitation.** As described previously (3), cultures in T-75 flasks were exposed to 500 μCi of [$^3$H]leucine (120 Ci/mmol) per ml for 30 min. Cell extracts were prepared and immunoprecipitated with absorbed goat anti-p15 (gag) serum, following which the immunoprecipitates were analyzed by electrophoresis on 0.1% SDS-8% polyacrylamide gels, dried, and autoradiographed.

**Cellular RNA isolation and S1 analysis.** To measure MuSVts110 RNA splicing at various growth temperatures, we followed our previous protocol (11). The cells were first grown at 33°C to about 75% confluency, and then shifted overnight to either 28, 37, or 39°C. Total cellular RNA was isolated from these cells with RNAzol B (Biotecx Laboratories, Inc.) as recommended by the supplier. S1 analyses with a 5′ end-labeled wt probe capable of measuring ligation at the MuSVts110 3′ ss were carried out as described previously (35, 36, 56). In all of these analyses, conditions were adjusted such that S1 nuclease did not digest the wt probe-mutant RNA hybrids.

In some experiments, a RNase protection assay was used to measure splicing efficiency (22). In this assay, we subcloned the probe that was employed in the S1 analyses (56) into pGEM-7Zf (Promega). To generate antisense RNA, the plasmid DNA was linearized with *Xba*I and transcribed with T7 RNA polymerase in the presence of [α-$^{32}$P]UTP. The resulting 159-nucleotide RNA was gel purified and hybridized to 10 to 50 μg of cellular RNA at 50°C for at least 8 h. The hybrid was digested with RNase A and T1 in the presence of 300 mM NaCl to prevent RNase digestion at single base mismatches, (22) and was analyzed on a 5% polyacrylamide gel containing 8 M urea. Unspliced MuSVts110 RNA will protect 139 bases of this probe, while the spliced RNA will protect 89 bases. Since there are 21 and 11 uridine residues in the 139- and 89-base protection fragments, respectively, a correction factor was applied to estimate splicing efficiency.

**In vitro splicing.** The MuSVts110 minitranscript used for in vitro splicing was based on the splicing-competent BB exon double deletion mutant of MuSVts110 (56). To generate BB, MuSVts110 DNA was digested with *Bsm*I-*Bal*I, and the 1,060-nucleotide internal fragment containing 336 nucleotides of E1, the 431-nucleotide intron, and 293 nucleotides of E2 was isolated. This fragment was originally subcloned into the *Sma*I site of pGEM-3Z (Promega) but has since been excised with *Sac*I-*Hin*dIII and inserted into similarly cut pBluescript II KS (Stratagene). For in vitro transcription with T7 polymerase, the BB-pBluescript plasmid DNA was linearized with *Cla*I. When vector nucleotides at the 5′ and 3′ ends are included, the BB transcript is 1,119 nucleotides in length. The mutants pBB:G(−25)A, pBB:G(−25)A,U(−27)C, and pBB:19Y-4U were linearized with *Hin*dIII for in vitro transcription with T7 RNA polymerase. Radiolabeled transcripts were synthesized in vitro by using 20 U of T7 RNA polymerase, 0.5 mM each nucleoside triphosphate, 25 μCi of $^{32}$P-labeled UTP (800 Ci/mmol), and the dinucleotide primer G(5′)ppp(5′)G. The transcripts were purified by elution in 0.5 M ammonium acetate–2.5 mM EDTA–1% SDS from a 4% polyacrylamide–7.5 M urea gel run in TBE buffer.

Nuclear extracts were prepared from HeLa S3 cells grown in RPMI 1640 medium (Life Technologies) containing 10% bovine calf serum and supplemented with 0.25% D-glucose. Extracts were prepared as described by Dignam et al. (13) and modified by Black (5). In vitro splicing was carried out in a 10-μl reaction volume containing $^{32}$P-labeled RNA precursor (approximately $10^5$ cpm), 20 mM creatine phosphate, 2.0 mM ATP, 2.0 mM $MgCl_2$, 2% polyethylene glycol, 1.2 mM dithiothreitol, and 50% (vol/vol) nuclear extract. Incubations were carried out at 30°C for 0 to 2 h.

**BP mapping.** Reverse transcriptase-driven primer extension (5′ end-labeled JEFF1 primer [5′AGGACCGCGAGTCTACCG-3′; MuSVts110 nucleotides 2561 to 2578]) was carried out on the total product from a 10-μl splicing reaction mixture in the presence of 100 mM Tris (pH 8.3), 12 mM $MgCl_2$, 10 mM dithiothreitol, 0.5 mM of each deoxynucleoside triphosphate, and 8 U of avian myeloblastosis virus (AMV) reverse transcriptase (Promega). The product of the reactions were visualized on a 6% polyacrylamide–7.5 M urea gel. A portion of the $^{32}$P-labeled primer was used to sequence pBB.G(−25)A DNA for a marker.

Debranching was carried out as described by Ruskin and Green (46). Briefly, the product of a 10-μl splicing reaction mixture was incubated in 19 μl of buffer D (20 mM *N*-2-hydroxyethylpiperazine-*N*′-2-ethanesulfonic acid [HEPES; pH 7.9], 20% glycerol, 100 mM KCl, 0.5 mM dithiothreitol, and 8 mM EDTA), 5 μl of S100 HeLa cell cytoplasmic extract (11), and 1 μl of RNAsin (Promega; 40 U/μl) for 30 min at 4°C. The debranched product was then phenol-chloroform extracted and analyzed on a 4% polyacrylamide–7.5 M urea gel.

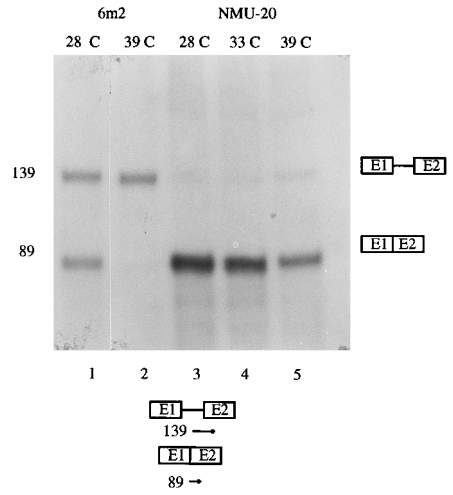


FIG. 1. MuSVts110 RNA splicing in the NMU-20 revertant. Cellular RNA was isolated from NMU-20 cells at 28, 33, and 39°C as well as from control 6m2 cells at 28 and 39°C. S1 analysis with the 5′-end-labeled pBAcc probe was carried out on 10 μg of each RNA preparation.

## RESULTS

**Induction of the NMU splicing phenotype in 6m2 cells.** We previously reported that treatment of MuSVts110-infected cells (6m2 cells) with 10 μM to 1 mM NMU resulted in a dose-dependent outgrowth of stably transformed foci at 39°C. In these NMU revertants, MuSVts110 RNA was spliced to virtual completion at all growth temperatures, resulting in the constitutive production of p85$^{gag\text{-}mos}$ (4, 8) whose presence explained the continuous maintenance of the transformed phenotype at 39°C. In contrast, untreated 6m2 cells remained contact inhibited and morphologically normal at 39°C, becoming senescent after prolonged cultivation, since at this growth temperature MuSVts110 RNA is not spliced and p85$^{gag\text{-}mos}$ cannot be produced. An example of the typical, nearly complete NMU revertant splicing pattern is shown for the representative NMU-20 revertant (Fig. 1, lanes 3 to 5) and differs sharply from the wt MuSVts110 splicing phenotype (Fig. 1, lanes 1 to 2) in which viral RNA splicing is generally no greater than 50% efficient at 33°C and essentially absent at 39°C. The consequence of constitutive MuSVts110 RNA splicing is, as noted above, the unrestricted production of p85$^{gag\text{-}mos}$. Examples of p85$^{gag\text{-}mos}$ production for the NMU-17, -18, -20, and -21 revertants are shown in Fig. 2A (lanes 1 to 8) and stand in contrast to the progressive decrease in p85$^{gag\text{-}mos}$ production as a function of growth temperature in the control MuSVts110-infected cells (Fig. 2B, lanes 1 to 4).

**Mutations in the MuSVts110 DNA in NMU-20 cells.** As noted above, we have reported that MuSVts110 RNA splicing is regulated in *cis* by sequences residing in two separate regions of the transcript: one (the E2DE) located in the v-*mos* exon, and the other involving the BP signal (11, 56). With this in mind, approximately 2 kb of the integrated MuSVts110 DNA

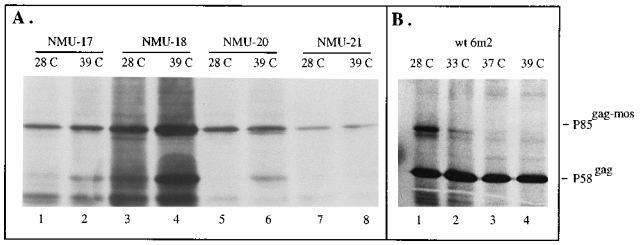


FIG. 2. Viral protein expression in NMU revertants. Radiolabeled cell extracts from control 6m2 cells and the NMU-17, -18, -20, and -21 revertants were treated with anti-p15, and the immunoprecipitates were analyzed on 8% polyacrylamide gels containing SDS. (A) Viral protein expression in the NMU revertants. (B) Viral protein expression in control 6m2 cells.

in NMU-20 cells (termed tsNMU-20 DNA), extending from about 100 nucleotides upstream of the 5′ ss through the end of the *mos* exon, were amplified with a series of overlapping primers (Fig. 3) and screened by SSCP, a technique that relies on conformation-induced differences in the electrophoretic mobility of wt and mutant DNA fragments (39, 40). SSCP identified several possible mutations in tsNMU-20 DNA, the cleanest example of which was a mutation in the vicinity of the 3′ ss detectable by most, but not all, primer pairs spanning this region. For example, 6m2 (wt MuSVts110) and tsNMU-20 DNA fragments amplified with either the JT6/CH1 or JT5-J1 primer pairs migrated markedly differently (Fig. 3, lanes 4 and 5 and 6 and 7), suggesting that a mutation lay between nucleotides 2377 and 2504 in tsNMU-20 DNA (the 3′ ss is at nucleotide 2476); however, no mobility shift was observed between 6m2 and tsNMU-20 fragments amplified with the JT5-CH2 primers (Fig. 3, lanes 2 and 3). Sequencing identified four scattered NMU-induced nucleotide substitutions (Fig. 4). In the intron (nucleotides 2046 to 2476), a G-to-A transition was found at nucleotide 2452. This mutation, termed G(−25)A,

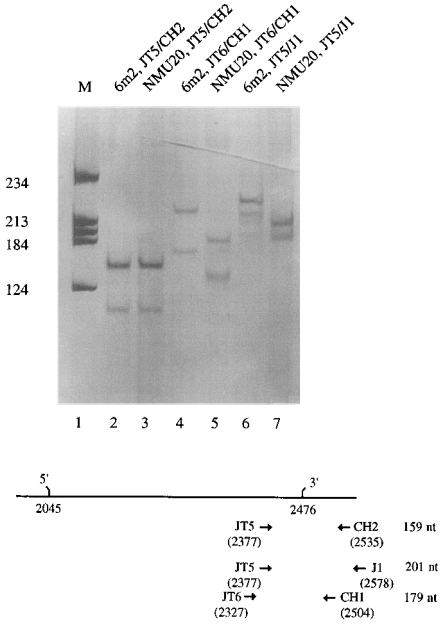


FIG. 3. SSCP analysis of tsNMU-20 DNA. Cellular DNA from NMU-20 or control 6m2 cells was amplified with the MuSVts110-specific primer pairs indicated and analyzed on a 9% polyacrylamide gel under nondenaturing conditions. Lane 1 (M), a pBR322/*Hae*III marker. nt, nucleotide.

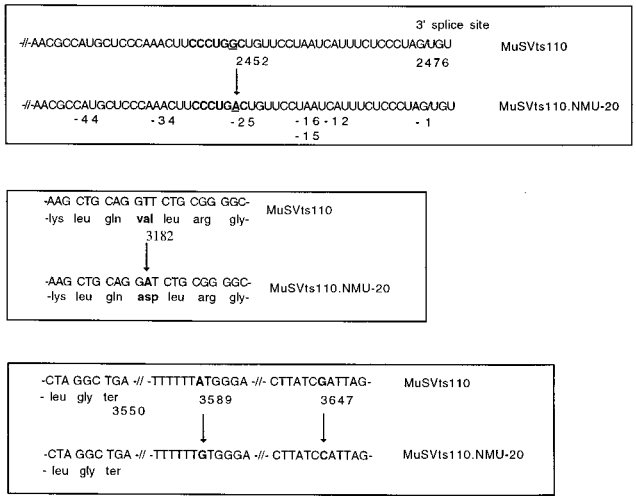


FIG. 4. Mutations in tsNMU-20 DNA. DNA sequencing was performed on amplified fragments of tsNMU-20 DNA. Mutations were found in four locations: a substitution of A for G at nucleotide 2452 (top box), a substitution of A for T at nucleotide 3182 (middle box), and substitutions of G for A and C for G at nucleotides 3589 and 3647, respectively (bottom box).

was within the 3′ ss-containing region displaying altered mobility by SSCP and was predicted to have two effects. First, it generated a strong BP signal at −25 relative to the 3′ ss (altering -CCCUG**G**C- to -CCCUG**A**C-) and, hence, would be predicted to have an effect on splicing. Second, it converted a -UGG- codon to a -UGA- stop codon and should have shortened the $p58^{gag}$ translation product by 8 amino acids but would have no effect on the $p85^{gag\text{-}mos}$ protein since this lies within its intron. In the v-*mos* region, a T-to-A transversion was found at nucleotide 3182, predicting a change from valine to aspartic acid in $p85^{gag\text{-}mos}$. Finally, in the untranslated region between the v-*mos* and U3 region of the 3′ long terminal repeat, two other substitutions were found: A to G at nucleotide 3589 and G to C at nucleotide 3647.

**Mutations conferring the NMU splicing phenotype.** We focused on the G(−25)A "gain-of-BP" mutation as being most likely responsible for the NMU splicing phenotype, since, as noted above, insertion of a β-globin BP into a splicing-incompetent MuSV mutant can activate efficient, nonthermosensitive splicing that is very similar to the splicing pattern exhibited in NMU-20 cells (11). To test whether the G(−25)A mutation explained the unrestricted splicing phenotype, a tsNMU-20 intron cassette containing only the G(−25)A mutation was amplified from NMU-20 cellular DNA, sequenced to confirm the presence of a single mutation, and inserted into wt MuSVts110 DNA (the MuSVts110 intron is defined here as a region defined by *Xho*I and *Acc*I sites, containing 35 nucleotides of E1, the entire 431-nucleotide intron, and 88 nucleotides of E2). This chimera [MuSVts110.G(−25)A] was stably transfected into NIH 3T3 cells, and its splicing phenotype was assessed by S1 analysis. As shown, MuSVts110.G(−25)A RNA was spliced to virtual completion (95 to 99%) at both 28 and 39°C (Fig. 5; compare lanes 4 and 5 with lanes 2 and 3), arguing that the G(−25)A mutation was fully responsible for the acquisition of the NMU splicing phenotype. As indicated in Materials and Methods, the S1 assay conditions were adjusted such that hybrids formed between the wt probe and mutant RNA were not spuriously digested at the mismatched positions. In the case of the G(−25)A and G(−25)A,U(−27)C RNAs, spurious digestion would have resulted in the appear-

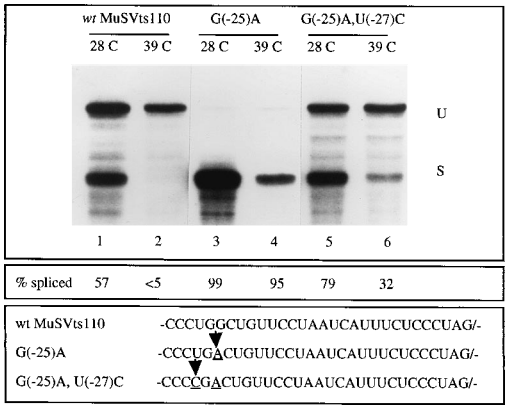


FIG. 5. The MuSVts110.G(−25)A splicing phenotype in vivo. Cellular RNA was isolated from control 6m2 cells growing at 28 and 39°C and NIH 3T3 cells transfected with MuSVts110 RNA carrying the G(−25)A mutation [termed MuSVts110.G(−25)A]. RNase protection was carried out as described in Materials and Methods. Lanes: 1 and 2, 6m2 RNA; 3 and 4, RNA from NIH 3T3 cells transfected with MuSVts110.G(−25)A DNA; 5 and 6, RNA from NIH 3T3 cells transfected with MuSVts110.G(−25)A,U(−27)C DNA. U, unspliced RNA; S, spliced RNA.

ance of a 104-nucleotide protection fragment which was not seen in any of the nuclease protection assays (e.g., Fig. 1 and 5).

There is good evidence that the balance maintained between unspliced and spliced retroviral RNAs is the net result of the relative strengths of suboptimal splicing signals at the 3′ splice site (7, 15, 26, 27, 32, 67). Since the G(−25)A BP (-CCCUG AC-) was an excellent match to the mammalian BP consensus sequence (-YNYURAC-), it was not unexpected that it might support efficient splicing at the permissive temperature. However, it was very interesting that the splicing of viral pre-mRNAs carrying this BP was not inhibited at high growth temperatures, and this suggested that this novel splicing phenotype might be conferred by a weak conserved splicing signal rather than by some more unique mechanism. To ask directly whether the strength of the G(−25)A BP was related to splicing thermosensitivity, we lessened its complementarity to U2 snRNA by a U-to-C mutation at position 4 [CCCUGAC to CCCCGAC, which was termed G(−25)A,U(−27)C]. In both avian retroviral and cellular pre-mRNAs, changes at position 4 in the BP consensus sequence markedly reduce splicing efficiency, frequently by blocking spliceosome maturation (16, 44, 49), and have been reported in one case to inhibit the second splicing reaction specifically (7). As shown, the G(−25)A,U(−27)C mutation reduced MuSVts110 splicing efficiency at the permissive temperature moderately (to about 80%) (Fig. 5; compare lanes 4 and 6). However, at 39°C, the G(−25)A,U(−27)C mutation was much more inhibitory, reducing splicing efficiency sharply (to about 30%) (Fig. 5; compare lanes 5 and 7). This partially thermosensitive splicing phenotype is intermediate between the virtually complete, temperature-independent splicing observed in MuSVts110 RNA carrying the G(−25)A mutation, and the 40 to 60% efficient, fully temperature-sensitive splicing exhibited by wt MuSVts110. These results argue that MuSVts110 splicing thermosensitivity is directly related to the degree to which the BP conforms to the mammalian consensus.

**MuSVts110 polypyrimidine tract mutants.** It is well established that binding of U2AF to the polypyrimidine tract stabilizes the interaction of U2 snRNA with the BP (29, 66). Moreover, studies of U2AF interaction with the polypyrimidine tract have shown that the factor has a distinct binding preference for stretches of five uridines (45). Since the tract of consecutive pyrimidines in the MuSVts110 polypyrimidine tract (-UUUC UCCCUAG/-) is short and contains a stretch of only 3 consecutive uridines, we asked whether lengthening and/or providing more consecutive uridines in the tract would alter balanced splicing and/or splicing thermosensitivity. Initially, three A-U mutations were introduced at −12, −15, and −16 relative to the 3′ ss. These mutations linked the wt MuSVts110 polypyrimidine tract to an upstream cluster of pyrimidines, yielding a tract containing 19 pyrimidines within which was a stretch of four consecutive uridines (Fig. 6C; 19Y-4U). These mutations had a marked effect on MuSVts110 splicing in vivo; splicing efficiency rose from 44 to 72% at the permissive temperature and from negligible levels to about 56% at the nonpermissive temperature (Fig. 6A, lanes 2 and 3; Fig. 6C). Since the U2AF binding site in the 19Y-4U polypyrimidine tract was still theoretically suboptimal, we tested the possible additive effect of an optimal U2AF binding site by introducing a C-to-U mutation at −13, generating a 19-residue polypyrimidine tract containing 9 consecutive uridines (Fig. 6C; 19Y-9U). The additional effect of this mutation could not be considered significant; the splicing efficiencies of 19Y-9U RNA were 76 and 58% at the permissive and nonpermissive temperatures, respectively (Fig. 6B, lanes 3 and 4; Fig. 6C). Note that in both these triple and quadruple polypyrimidine tract mutants, spurious nuclease cleavage of unspliced RNA was noted at the mismatched positions commencing 12 nucleotides from the 3′ ss. (Fig. 6A and B [designated U*]). In calculating splicing efficiency, the radioactivity in the U* bands was considered to be unspliced RNA.

**In vitro splicing of MuSVts110 minitranscript BP and polypyrimidine tract mutations.** In vitro splicing experiments were carried out to determine which steps in splicing were most affected by the mutations introduced. Moreover, it was necessary to test whether the G(−25)A BP was actually being utilized as predicted, although the reduction in splicing efficiency

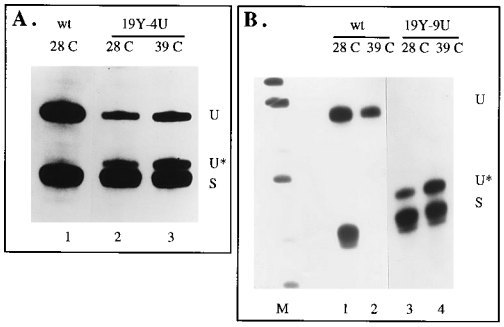


C.

| Mutant | PPT sequence | Splicing Efficiency (%) 28 C | 39 C |
|---|---|---|---|
| 9Y-3U (wt) | -UUCCUAAUCAUUUCUCCCUAG/- | 44 | - |
| 19Y-4U | - UUCCUUUUCUUUUCUCCCUAG/- | 72 | 56 |
| 19Y-9U | - UUCCUUUUUUUUUCUCCCUAG/- | 76 | 58 |

FIG. 6. Splicing of MuSVts110 polypyrimidine tract mutants in vivo. Otherwise wt MuSVts110 DNAs containing the 19Y-4U and 19Y-9U mutations were transfected into NIH 3T3 cells. RNA was isolated from these cells at 28 and 39°C, and splicing efficiency was estimated by S1 analysis. (A) Splicing of the MuSVts110 19Y-4U mutant RNA. (B) Splicing of the MuSVts110 19Y-9U mutant RNA. wt, wt MuSVts110 RNA; M, marker lane; U*, unspliced RNA spuriously digested at the wt probe-mutant polypyrimidine tract mismatch; S, spliced RNA. (C) Sequence and splicing efficiency of polypyrimidine tract (PPT) mutants.

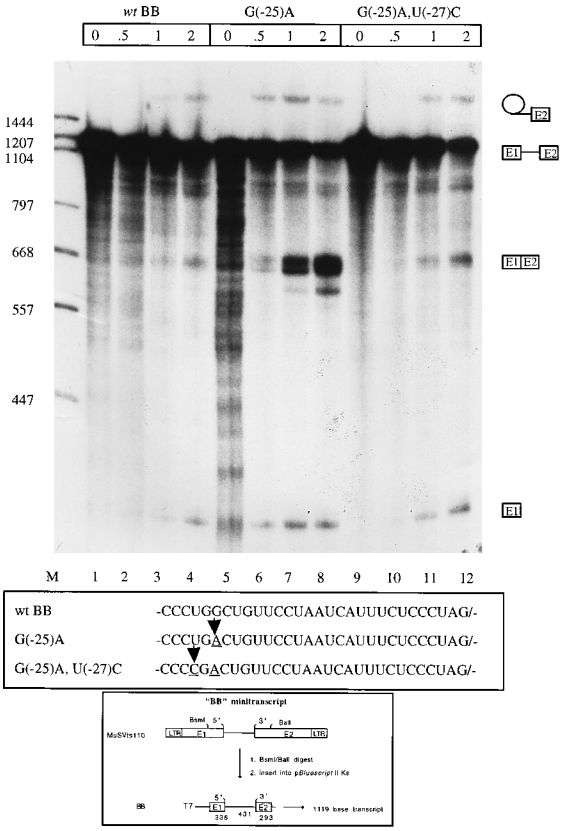


FIG. 7. In vitro splicing of BB, BB.G−25A, and BB.G(−25)A,U(−27)C transcripts. For in vitro splicing, [$^{32}$P]UTP-labeled minitranscripts were incubated in nuclear extracts as indicated in Materials and Methods. Aliquots were removed at various times, phenol extracted, and analyzed by gel electrophoresis. 0, 0.5, 1, and 2, 0, 30, and 120 min, respectively. Lane 1 (M), RSV-*Taq*I marker. The positions of branched intermediates, pre-mRNA, ligated exons, and exon 1 are indicated on the right. The sequences of wt MuSVts110, G(−25)A, and G(−25)A,U(−27)C RNAs in the BP region are shown at the bottom.

seen as a consequence of the G(−25)A,U(−27)C mutation argued strongly for its use as a BP.

For the in vitro splicing experiments, we used a MuSVts110-based minitranscript, termed BB, in which the *gag* and *mos* exons were reduced to 250 to 300 nucleotides each (diagrammed at the bottom of Fig. 7). Previously, we had shown that BB viral RNA is spliced at about 65% efficiency in transfected cells (56), making it an attractive candidate as an in vitro splicing substrate. Nonetheless, BB RNA was very poorly spliced in vitro. Over a 120-min incubation period, its conversion to RNA species whose mobility and size were consistent with branched intermediates and free E1 was slow (these species were not detectable prior to 1 h of incubation in splicing extracts), and very little exon ligation was observed. These kinetics indicated the presence of a block prior to the first splicing reaction that was very similar to the block previously reported for wt ASV RNA splicing (15, 26, 27) (Fig. 7, lanes 2 to 5). Introduction of the G(−25)A mutation both accelerated the appearance of the presumed branched intermediate and E1 (these could readily be detected by 30 min of incubation) and resulted in a very large increase in exon ligation (Fig. 7, lanes 6 to 9), again very much like the effect of linker-inserted BP sequences near the ASV *env* gene 3′ ss and, in addition, extremely similar to the effect on splicing observed in vivo in cells transfected with MuSVts110.G(−25)A DNA (Fig. 5). However, somewhat surprisingly given the relatively moderate reduction in splicing efficiency at the permissive temperature caused by combining the G(−25)A and U(−27)C mutation in vivo, introduction of the U(−27)C mutation into BB RNA carrying the G(−25)A BP reduced splicing efficiency in vitro sharply. In G(−25)A,U(−27)C RNA, both the lariat intermediate and E1 appeared late and tended to accumulate, and exon ligation was sharply reduced to levels only slightly higher than those observed in the wt transcript (Fig. 7, lanes 11 to 13). These kinetics were very similar to those of wt BB RNA and argued for the reinstatement of the blockade prior to the first splicing reaction.

We also assessed the effect of the 19Y-4U polypyrimidine tract mutation on BB splicing in vitro. As noted above, in vivo this mutation caused an approximate doubling of splicing efficiency and a very marked lessening in splicing thermosensitivity (Fig. 6). However, 19Y-4U RNA was spliced only slightly more efficiently than the wt BB and G(−25)A,U(−27)C RNAs in in vitro splicing extracts (Fig. 8; compare lanes 1 to 4 and 13 to 16), once again arguing for the presence of a block at or prior to the first splicing reaction. These observations indicated that the stronger polypyrimidine tract, while a very positive influence on MuSVts110 splicing in vivo, was in vitro unable to provide compensatory functions similar to those of a consensus BP.

The disparate, although parallel, splicing efficiencies observed for the various MuSVts110 splicing substrates in vivo and in vitro emphasize the difficulty of making direct comparisons between these sets of conditions. BB viral RNA (in which the truncated exons remain between viral long terminal repeats) is spliced at about 65% efficiency at permissive temperatures in vivo but in minitranscript form is very poorly spliced in vitro. Provision of the G(−25)A BP in wt MuSVts110 permits approximately 98% splicing at all temperatures in vivo and approximately 50% splicing in BB RNA in vitro, suggest-

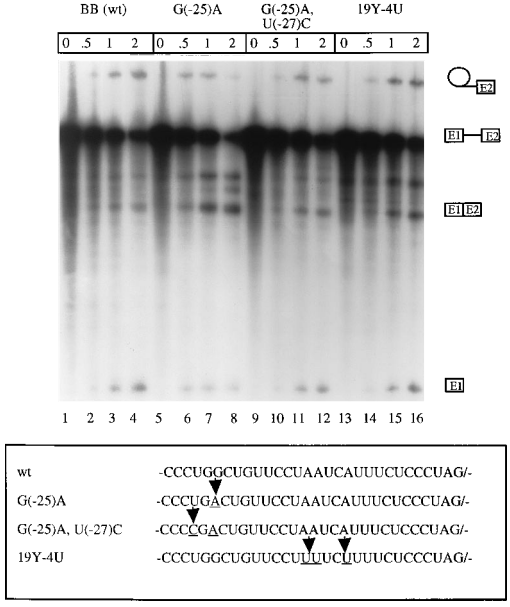


FIG. 8. In vitro splicing of the polypyrimidine tract mutant 19Y-4U. In vitro splicing was carried out as described in the legend to Fig. 7. 0, 0.5, 1, and 2, 0, 30, 60, and 120 min, respectively. The migration positions of branched intermediates, pre-mRNA, ligated exons, and exon 1 are indicated to the right. The sequences in the vicinity of the 3′ ss of wt MuSVts110, G(−25)A, G(−25)A, U(−27)C, and 19Y-4U RNAs are shown below.

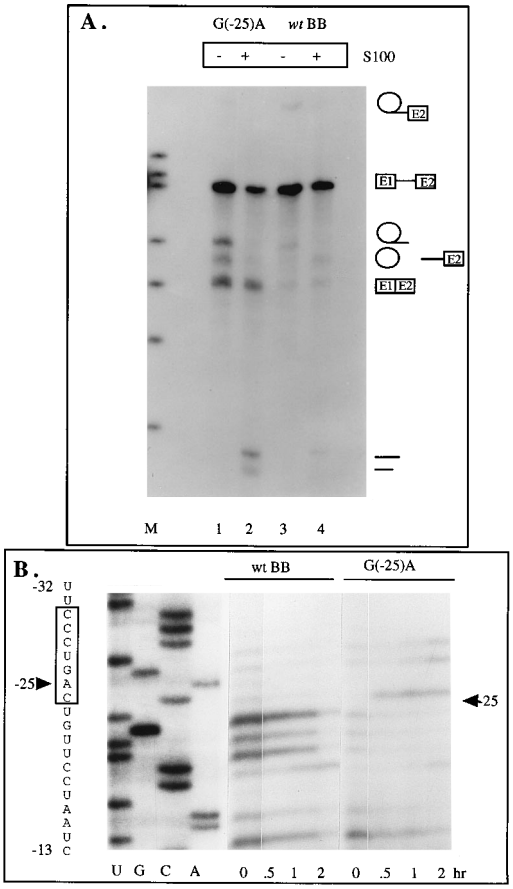


FIG. 9. Debranching and BP mapping. (A) Debranching carried out on the BB and BB:G(−25)A 120-min in vitro splicing products as described in Materials and Methods. Lanes: 1 and 2, BB:G(−25)A spliced product treated with debranching enzyme (+) or left untreated (−); 3 and 4, wt BB spliced product treated with debranching enzyme (+) or left untreated (−). (B) BP mapping carried out by reverse transcriptase blockading which was followed by gel electrophoresis as described in Materials and Methods. Samples were prepared from 0-, 0.5-, 1-, and 2-h wt BB and BB.G(−25)A RNA in vitro splicing products. The total in vitro splicing products were directly hybridized to the JEFF1 primer, which was extended with reverse transcriptase, and the extension products were analyzed by gel electrophoresis. As a sequence reference, BB.G(−25)A DNA was sequenced with the same primer and analyzed in parallel.

ing very strongly that the blockade to BB RNA splicing in vitro involves the BP-U2 snRNA interaction and/or its stabilization by U2AF. Since weakening the G(−25)A BP by a U(−27)C second-site mutation only moderately reduces splicing efficiency in vivo but drastically inhibits splicing in vitro, and since improving the polypyrimidine tract has a large positive effect in vivo but very little effect in vitro, we infer that the BP-U2 snRNA interaction is the critically affected step.

**Debranching and BP mapping.** The most slowly moving RNA species on gels containing in vitro splicing products was assumed to represent the branched intermediate. As a test, we treated the spliced products with debranching enzyme (46). As expected, after this treatment the most slowly moving RNA species disappeared from both the BB and BB.G(−25)A in vitro-spliced products (Fig. 9A), arguing that these were the branched intermediates. In addition, an RNA species of about 800 nucleotides in size also disappeared; we speculate that this represented the excised but still circular intron. An approximately 750-nucleotide species was resistant to debranching and very probably represents the linear intron-E2 RNA. The vanished species were replaced by an RNA tracking at approximately 430 nucleotides, which is the size expected for the linear intron (431 nucleotides), and a slightly smaller RNA species, which we suspect is the linearized remainder of a circular intron digested down to the BP by cellular nucleases.

In BB.G(−25)A RNA, it was expected that novel lariat formation would take place at the A residue located in the G(−25)A BP sequence. To map the location of the BP used, wt BB and BB.G(−25)A 0- to 2-h in vitro splicing products were analyzed by reverse transcriptase-driven primer extension. As expected, no primer extension blockades were observed at −25 at any time point in the wt BB product (Fig. 9B, BB). In addition, all blockades to the progress of reverse transcriptase observed in this region of the BB transcript were scattered and not restricted to A residues, which are further strong indications that they were unrelated to lariat formation. In BB.G(−25)A RNA, no reverse transcriptase blockade was observed at −25 at the zero time point [Fig. 9B, G(−25)A]; however, commencing at 30 min of incubation under splicing conditions and persisting through the 2-h point, a strong blockade to primer extension was observed at −25 [Fig. 9B, G(−25)A]. From the absence of this blockade in the wt BB splicing product and its appearance in the BB.G(−25)A splicing product coincident with the appearance of the branched intermediate during splicing (Fig. 7), we concluded that this blockade represented BP formation at −25.

## DISCUSSION

A growing literature indicates that retroviral pre-mRNA, some of which must remain unspliced and reach the cytoplasm for the translation of *gag* and *gag-pol* products and for packaging into virions, escapes splicing through the tenuous interaction of suboptimal splicing signals at the 3′ ss with spliceosome components (2, 7, 15, 26, 27, 32, 49, 55, 57, 58, 67). These weak interactions are abetted by other *cis*-acting signals in retroviral exons and introns (1a, 19, 27, 33). Hence, simple retroviral RNAs differ from most cellular RNAs in that their splicing is neither all or none nor obligatorily coupled to nuclear transport.

Several previous studies have shown that a suboptimal BP is a major contributor to balanced avian retroviral RNA splicing. Conversion of the wt ASV *env* gene BP to a near-consensus BP by insertion of a linker oligonucleotide or to a consensus β-globin BP by direct mutagenesis induces oversplicing at the *env* gene 3′ ss (26). The importance of maintaining the proper balance between unspliced and spliced RNA species during retroviral replication is emphasized by the fact that this consensus BP-induced oversplicing confers a replication defect due to an insufficiency of unspliced RNA for the production of viral structural gene products, enzymes, and infectious virions. Oversplicing caused by linker insertion was determined to be caused by the introduction of two overlapping BPs (-AGCU UAGAG-) and could be suppressed by a U-to-C mutation at position 4 in the upstream BP (-AGCCUAGAG-) (15, 26, 27). Interestingly, this suppressor mutation appears to block the second step in splicing and can itself be suppressed by extension of the polypyrimidine tract just downstream of the BP as well as reinstated after reversal by a C-for-U mutation in the probable U2AF binding site in the polypyrimidine tract (7).

Our results with MuSVts110 present an interesting parallel with those for ASV. In an earlier study, we demonstrated that insertion of a β-globin BP near the 3′ ss in a splicing-negative MuSVts110 mutant induced highly efficient, nonthermosensitive splicing (11). The current results confirm and considerably extend the earlier findings and, in addition, have the advantage

of arising from mutations that were far less context altering than those introduced in our earlier work. In the NMU-20 MuSVts110 revertant studied here, a G-to-A point mutation [G(−25)A] creating a consensus BP (-CCCUG**A**C-) at −25 relative to the 3′ ss was the critical alteration. Viral RNA containing this BP was, like most cellular pre-mRNAs, spliced to virtual completion at all growth temperatures. In the ASV system, the introduction of consensus (7) and the introduction of near-consensus BPs (26, 27) near the *env* gene 3′ ss have been demonstrated to have qualitatively similar effects. Differences in the magnitude of the effect of consensus BP insertion in the ASV and MuSVts110 retroviruses (e.g., oversplicing versus complete splicing) can very probably be explained by the fact that the MuSVts110 G(−25)A BP (-CCCUGAC-) is a slightly better match for the mammalian consensus (-YNYU RAC-) than the linker-inserted ASV BP (-AGCUUAG-), is at a different distance from the 3′ ss, and is paired with a polypyrimidine tract with a different length and pyrimidine content. Moreover, the effects of position 4 mutations in the active BPs are comparable; in ASV, a U-to-C mutation (T/C −20°) at position 4 suppressed oversplicing, and in MuSVts110, a U-to-C mutation at the cognate position [U(−27)C] in the G(−25)A BP reduced splicing moderately at the permissive temperature and restored a substantial amount of splicing thermosensitivity. Similar results have been reported for AMV and HIV-1. In a temperature-sensitive transformation mutant of AMV, a C-for-U mutation at position 4 (-GAU**U**AAU- to -GAU**C**AAU-) was found in a BP consensus sequence very probably used in the splicing of the *myb* RNA (49). The weaker BP caused a substantial overall reduction in splicing efficiency and, thus, lower amounts of Myb protein. In HIV, a recent study examined the strength of splicing signals near the inefficiently used *tat*/*rev* 3′ splice site. It was found that altering the sequence near the 3′ splice site to mimic a globin gene BP signal produced a dramatic increase in splicing efficiency (55).

Our experiments implicate a weak BP signal in wt MuSVts 110 splicing thermosensitivity. While the wt MuSVts110 BP has not yet been unequivocally identified, we have narrowed the possibilities by assessing the in vivo splicing efficiency of MuSVts110 RNAs in which BP A's located in near-consensus BP sequences at −12, 15, −16, −34, −35, 36, −44, and −113/−114 relative to the MuSVts110 3′ ss were mutated. Our preliminary data indicate that the BP(s) at −113/−114 as well as at least one in the cluster between −34 and −44 is active but that the potential BPs at −12, −15, and −16 are inactive (14a). This conclusion is supported by the observation in the present study that mutation of the adenosine residues at −12, −15, and −16 to U in extending the polypyrimidine tract greatly increased rather than reduced splicing efficiency, but it must be qualified by the possibility that a strong polypyrimidine tract might recruit an otherwise cryptic BP.

**MuSVts110 polypyrimidine tract.** In avian retroviruses and HIV, the polypyrimidine tract has been shown to contribute to balanced splicing. In ASV, for example, mutations in the polypyrimidine tract can mitigate the replication defect caused by oversplicing at the *env* 3′ ss (7). Moreover, much like the provision of a near-consensus BP in ASV, strengthening the RSV *src* gene polypyrimidine tract can cause oversplicing at the *src* 3′ ss and a concomitant replication defect due to an insufficient amount of unspliced RNA (67). The virtually complete splicing at all growth temperatures of MuSVts110 RNA containing a consensus BP suggests that the wt MuSVts110 polypyrimidine tract, despite its minimal length and lack of uridine stretches favorable for U2AF binding, is fully functional when paired with a consensus BP. In our previous work, full function of the wt MuSVts110 polypyrimidine tract could be inferred from the efficient splicing obtained after insertion of a β-globin BP (11). Moreover, in wt ASV, insertion of a globin BP has a similar positive effect on splicing, indicating the competence of the polypyrimidine tract in this avian retrovirus as well (7). In the present work, extending the length of the MuSVts110 polypyrimidine tract caused a striking increase in splicing efficiency and lessening of splicing thermosensitivity that was not significantly enhanced by the additional provision of an optimal U2AF binding site. In this connection, it should be emphasized that during splicing the polypyrimidine tract interacts with several splicing factors in addition to U2AF, among them the polypyrimidine tract binding protein (17, 18, 41) and its associated factor (PSF) (42) and an intron-binding protein (61). There is considerable evidence of a positive connection between overall length, the length of embedded U2AF-binding uridine tracts, and polypyrimidine tract function (34, 43, 45). It seems probable that the enhancement of in MuSVts110 splicing observed in the 19Y-4U and 19Y-9U mutants might be due to an improved interaction with one or more of these factors. These observations are very similar to those reported for ASV, in which the addition of two pyrimidines to the polypyrimidine tract could compensate for a mutation in the BP, but differ in one particular, since five consecutive uridines seemed to be required for the full functional activity of the slightly shorter polypyrimidine tract in ASV (7).

**Implications for splicing thermosensitivity.** Our current results demonstrate that both MuSVts110 splicing efficiency and thermosensitivty are sensitive to the strength of the BP signal and the length and uridine content of the polypyrimidine tract, suggesting that the virtually complete inhibition of MuSVts110 RNA splicing at physiological and higher growth temperatures may represent a stress response of a splicing substrate evolved for inefficient processing even under optimal conditions. At permissive temperatures, MuSVts110 pre-mRNA will splice at 30 to 50% efficiency; our previous and current findings indicate that the balance between unspliced and spliced MuSVts110 RNA is regulated in *cis* by suboptimal signals at the 3′ ss, as is the case for several other retroviral RNAs. Since splicing thermosensitivity in MuSVts110 is relaxed by the same alterations in splicing signals that regulate balanced splicing, it seems most probable that under suboptimal conditions (e.g., elevated growth temperatures), thermosensitive splicing results from a shift of the balance virtually completely toward escape from splicing. Ineffective base pairing between the wt MuSVts110 BP signal and U2 snRNA, exacerbated by a suboptimal polypyrimidine tract with a probably poor affinity for U2AF and other polypyrimidine tract-binding proteins, may be the underlying mechanism. This possibility is supported by our current results showing the loss of splicing thermosensitivity by provision of a consensus BP and its reinstatement when this BP is weakened, as well as by the results of two previous studies, one in which an inserted β-globin BP caused a similar loss of splicing thermosensitivity (11) and another in which duplication of the region surrounding the MuSVts110 3′ ss caused a loss of splicing thermosensitivity mediated by the fortuitous introduction of a near-consensus BP (-CUCUAAG-) just upstream of the duplicated 3′ ss (8). While the wt MuSVts110 BP has not yet been mapped, all of the potential BP sequences identified in preliminary work are either not well-matched to the consensus sequence or are distant from the 3′ ss. Hence, the interaction of any of these BPs with U2 snRNA and their contribution to the selection of the 3′ ss might be expected to be less than optimal. Moreover, the most likely binding site (-UUU-) for U2AF in the MuSVts110 polypyrimidine tract is weak; U2AF strongly prefers a binding site of five consecutive uridine residues (45). This combination of suboptimal BP and polypyri-

midine tract may explain why MuSVts110 RNA splicing is thermosensitive and why ASV RNA splicing, for example, has no known thermosensitive component. Both wt retroviruses utilize suboptimal BPs; however, the ASV polypyrimidine tract (-CCCUCUUUUUGCAG/-), unlike the MuSVts110 polypyrimidine tract (-UUUCUCCCUAG/-), contains an optimal U2AF binding site that we speculate may be far better able to stabilize the BP-U2 snRNA interaction. Interestingly, there is a third suboptimal splicing signal in MuSVts110 that contributes to splicing thermosensitivity. Mutation of position +6 in the MuSVts110 5′ ss (-CAG/GUAGGA-) to match the consensus sequence (-CAG/GUAGG**U**) results in a doubling in splicing efficiency and concomitant loss of splicing thermosensitivity (1). Position +6 is involved in commitment complex formation, since a uridine in this position enhances the U1 snRNP-promoted interaction of U2AF65 with the polypyrimidine tract (10). Moreover, a uridine at position +6 is optimal for both splicing reactions, since U6 snRNA forms critical base pairs with positions +5 and +6 in the 5′ ss (47, 48, 54, 62) during these reactions. Hence, the mispairing of position +6 in the MuSVts110 5′ ss with either U1 or U6 snRNA could contribute to the instability of the BP-U2 snRNA-BP interaction and/or reduce the efficiency of the splicing reactions.

## ACKNOWLEDGMENTS

This work was aided by the excellent technical assistance of Sandra A. Kinney and James Syrewicz.

This work was supported, in part, by grants from the National Cancer Institute (CA-34734) and the National Institutes of Environmental Health Services (ES-05323). Synthetic oligonucleotides were provided by Pamela O'Sullivan in the UTMDACC Macromolecular Synthesis and Analysis Facility, supported by core grant CA-16672 from the National Cancer Institute. J.W.T. and C.A.H. were supported in part by American Legion Auxiliary predoctoral fellowships.

## REFERENCES

1. **Ainsworth, J. R., L. M. Rossi, and E. C. Murphy, Jr.** Submitted for publication.
1a. **Arrigo, S., and K. Beemon.** 1988. Regulation of Rous sarcoma virus RNA splicing and stability. J. Virol. **8:**4858–4867.
2. **Berberich, S. L., and C. M. Stoltzfus.** 1991. Mutations in the regions of the Rous sarcoma virus 3′ splice sites: implications for regulation of alternative splicing. J. Virol. **65:**2640–2646.
3. **Biggart, N. W., G. A. Gallick, and E. C. Murphy.** 1987. Nickel-induced heritable alterations in retroviral transforming gene expression. J. Virol. **61:**2378–2388.
4. **Biggart, N. W., and E. C. Murphy.** 1988. Analysis of metal-induced mutations altering the expression or structure of a retroviral gene in a mammalian cell line. Mutat. Res. **198:**115–129.
5. **Black, D. L.** 1992. Activation of c-*src* neuron-specific splicing by an unusual element in vivo and in vitro. Cell **69:**795–807.
6. **Blair, D. G., M. A. Hull, and E. A. Finch.** 1979. The isolation and preliminary characterization of temperature-sensitive transformation mutants of Moloney sarcoma virus. Virology **95:**303–316.
7. **Bouck, J., X.-D. Fu, A. M. Skalka, and R. A. Katz.** 1995. Genetic selection for balanced retroviral RNA splicing: novel regulation involving the second step can be mediated by transitions in the polypyrimidine tract. Mol. Cell. Biol. **15:**2663–2671.
8. **Chiocca, S. M., D. A. Sterner, N. W. Biggart, and E. C. Murphy.** 1991. Nickel mutagenesis: alteration of the MuSVts110 splicing phenotype by a nickel-induced duplication of the 3′ splice site. Mol. Carcinog. **4:**61–71.
9. **Cizdziel, P. E., M. deMars, and E. C. Murphy.** 1988. Exploitation of a thermosensitive splicing event to study pre-mRNA splicing in vivo. Mol. Cell. Biol. **8:**1558–1569.
10. **Cote, J., J. Beaudouin, R. Tacke, and B. Chabot.** 1995. The U1 small ribonucleoprotein/5′ splice site interaction affects U2AF65 binding to the 3′ splice site. J. Biol. Chem. **270:**4031–4036.
11. **de Mars, M., P. E. Cizdziel, and E. C. Murphy, Jr.** 1990. Activation of cryptic splice sites in murine sarcoma virus-124 mutants. J. Virol. **64:**5260–5269.
12. **de Mars, M., D. A. Sterner, S. M. Chiocca, N. W. Biggart, and E. C. Murphy.** 1990. Regulation of RNA splicing in *gag*-deficient mutants of Moloney murine sarcoma virus MuSVts110. J. Virol. **64:**1421–1428.
13. **Dignam, J. D., R. M. Lebovitz, and R. G. Roeder.** 1983. Accurate transcription initiation by RNA polymerase II in a soluble extract from isolated nuclei. Nucleic Acids Res. **11:**1475–1489.
14. **Dominski, Z., and R. Kole.** 1991. Selection of splice sites in RNAs with short internal exons. Mol. Cell. Biol. **11:**6075–6083.
14a. **D'Souza, I., J. W. Touchman, and E. C. Murphy, Jr.** Unpublished observations.
15. **Fu, X.-D., R. A. Katz, A. M. Skalka, and T. Maniatis.** 1991. The role of branchpoint and 3′ exon sequences in the control of balanced splicing of avian retrovirus RNA. Genes Dev. **5:**211–220.
16. **Fu, X.-Y., H. Ge, and J. L. Manley.** 1988. The role of the polypyrimidine stretch at the SV40 early pre-mRNA 3′ splice site in alternative splicing. EMBO J. **7:**809–817.
17. **Garcia-Blanco, M. A., S. F. Jamison, and P. A. Sharp.** 1989. Identification and purification of a 62,000 dalton protein that binds specifically to the polypyrimidine tract of introns. Genes Dev. **3:**1874–1886.
18. **Gil, A. P., P. A. Sharp, S. F. Jamison, and M. A. Garcia-Blanco.** 1991. Characterization of cDNAs encoding the polypyrimidine tract-binding protein. Genes Dev. **5:**1224–1236.
19. **Gontarek, R. R., M. T. McNally, and K. Beemon.** 1993. Mutation of an RSV intronic element abolishes both U11/U12 snRNP binding and negative regulation of splicing. Genes Dev. **7:**1926–1936.
20. **Graham, R., and A. V. der Eb.** 1973. A new technique for the assay of infectivity of human adenovirus 5 DNA. Virology **52:**456–467.
21. **Hamelin, R. B., B. L. Brizzard, M. A. Nash, E. C. Murphy, and R. B. Arlinghaus.** 1985. Temperature-sensitive viral RNA expression in Moloney murine sarcoma virus *ts*110-infected cells. J. Virol. **53:**616–623.
22. **Hod, J.** 1992. A simplified ribonuclease protection assay. BioTechniques **13:**852.
23. **Horn, J. P., T. Wood, E. C. Murphy, D. G. Blair, and R. B. Arlinghaus.** 1981. A selective temperature-sensitive defect in viral RNA expression in cells infected with a ts transformation mutant of murine sarcoma virus. Cell **25:**37–46.
24. **Hwang, L. H.-S., J. Park, and E. Gilboa.** 1984. Role of intron-containing sequences in formation of Moloney murine leukemia virus *env* mRNA. Mol. Cell. Biol. **4:**2289–2297.
25. **Kandels-Lewis, S., and B. Seraphin.** 1993. Role of U6 snRNA in 5′ splice site selection. Science **262:**2035–2039.
26. **Katz, R. A., M. Kotler, and A. M. Skalka.** 1988. *cis*-Acting intron mutations that affect the efficiency of avian retroviral RNA splicing: implication for mechanisms of control. J. Virol. **62:**2686–2693.
27. **Katz, R. A., and A. M. Skalka.** 1990. Control of retroviral RNA splicing through maintenance of suboptimal processing signals. Mol. Cell. Biol. **10:**696–704.
28. **Konforti, B. B., M. J. Koziolkowicz, and M. M. Konarska.** 1993. Disruption of basepairing between the 5′ splice site and the 5′ end of U1 snRNA is required for spliceosome assembly. Cell **75:**863–873.
29. **Lee, C. G., P. D. Zamore, M. R. Green, and J. R. Hurwitz.** 1993. RNA annealing activity is intrinsically associated with U2AF. J. Biol. Chem. **268:**13472–13478.
30. **Lesser, C., and C. Guthrie.** 1993. Mutations in the U6 snRNA that alter splice site specificity: implifications for the active site. Science **262:**1982–1988.
31. **Lin, H., S. M. Chiocca, M. A. Gilbreth, J. A. Ainsworth, L. A. Bishop, and E. C. Murphy.** 1992. Moloney murine sarcoma virus MuSVts110: cloning, nucleotide sequence, and gene expression. J. Virol. **66:**5329–5337.
32. **McNally, M. T., and K. Beemon.** 1992. Intronic sequences and 3′ splice sites control Rous sarcoma virus RNA splicing. J. Virol. **66:**6–11.
33. **McNally, M. T., R. R. Gontarek, and K. Beemon.** 1992. Characterization of Rous sarcoma virus intronic sequences that negatively regulate splicing. Virology **185:**99–108.
34. **Mullen, M., C. W. J. Smith, J. G. Patton, and B. Nadal-Ginard.** 1991. Alpha-tropomyosin mutually exclusive exon selection: competition between branchpoint/polypyrimidine tracts determines default exon choice. Genes Dev. **5:**642–655.
35. **Nash, M., B. L. Brizzard, J. L. Wong, and E. C. Murphy, Jr.** 1985. Murine sarcoma virus *ts*110 RNA transcripts: origin from a single proviral DNA and sequence of the *gag-mos* junctions in both precursor and spliced viral RNAs. J. Virol. **53:**624–633.
36. **Nash, M., N. V. Brown, J. L. Wong, R. B. Arlinghaus, and E. C. Murphy.** 1984. S1 nuclease analysis mapping of viral RNAs from a temperature-sensitive transformation mutant of murine sarcoma virus. J. Virol. **50:**478–488.
37. **Newman, A. J., and C. Norman.** 1991. Mutations in yeast U5 snRNA alter the specificity of 5′ splice site cleavage. Cell **65:**115–123.
38. **Newman, A. J., and C. Norman.** 1992. U5 snRNA interacts with exon sequences at the 5′ and 3′ splice sites. Cell **68:**743–754.
39. **Orita, M., M. Iwahana, H. Kanezawa, K. Hayashi, and T. Sekiya.** 1989. Detection of polymorphisms of human DNA by gel electrophoresis as single-strand conformational polymorphisms. Proc. Natl. Acad. Sci. USA **86:**2766–2770.
40. **Orita, M., Y. Suzuki, T. Sekiya, and K. Hayashi.** 1989. Rapid and sensitive detection of point mutations and DNA polymorphisms using the polymerase chain reaction. Genomics **5:**874–879.

41. **Patton, J. G., S. A. Mayer, P. Tempst, and B. Nadal-Ginard.** 1991. Characterization and molecular cloning of a polypyrimidine tract-binding protein: a component of a complex necessary for pre-mRNA splicing. Genes Dev. **5:**1237–1251.
42. **Patton, J. G., E. B. Porro, J. Galceran, P. Tempst, and B. Nadal-Ginard.** 1993. Cloning and characterization of PSF, a novel pre-mRNA splicing factor. Genes Dev. **7:**393–406.
43. **Reed, R.** 1989. The organization of 3′ splice site sequences in mammalian introns. Genes Dev. **3:**2113–2123.
44. **Reed, R., and T. Maniatis.** 1988. The role of the branchpoint sequence in pre-mRNA splicing. Genes Dev. **2:**1268–1276.
45. **Roscigno, R. F., M. Weiner, and M. A. Garcia-Blanco.** 1993. A mutational analysis of the polypyrimidine tract of introns. J. Biol. Chem. **268:**11222–11229.
46. **Ruskin, B., and M. R. Green.** 1985. A RNA processing activity that debranches RNA lariats. Science **229:**135–140.
47. **Sawa, H., and J. Abelson.** 1992. Evidence for basepairing interaction between U6 small nuclear RNA and the 5′ splice site during the splicing reaction in yeast. Proc. Natl. Acad. Sci. USA **89:**11269–11273.
48. **Sawa, H., and Y. Shimura.** 1992. Association of U6 snRNA with the 5′ splice site region of pre-mRNA in the spliceosome. Genes Dev. **6:**244–254.
49. **Schirm, S., G. Moscovici, and J. M. Bishop.** 1990. A temperature-sensitive phenotype of avian myeloblastosis virus: determinants that influence the production of viral mRNAs. J. Virol. **64:**767–773.
50. **Seraphin, B. L., L. Kretzner, and M. Roshbash.** 1988. A U1 snRNA: pre-mRNA base pairing interaction is required early in spliceosome assembly but does not uniquely define the 5′ splice site. EMBO J. **7:**2533–2538.
51. **Siliciano, P. G., and C. Guthrie.** 1988. 5′ splice site selection in yeast. Genetic alterations in base pairing with U1 reveal additional requirements. Genes Dev. **2:**1258–1267.
52. **Smith, C. W. J., and B. Nadal-Ginard.** 1989. Mutually exclusive splicing of alpha-tropomyosin exons enforced by an unusual lariat branchpoint location. Cell **56:**749–758.
53. **Smith, C. W. J., E. B. Porro, J. G. Patton, and B. Nadal-Ginard.** 1989. Scanning from an independently specified branch point defines the 3′ splice site. Nature (London) **342:**243–247.
54. **Sontheimer, E., and J. A. Steitz.** 1993. The U5 and U6 small nuclear RNAs as active site components of the spliceosome. Science **262:**1989–1996.
55. **Staffa, A., and A. Cochrane.** 1994. The *tat*/*rev* intron of human immunodeficiency virus type 1 is inefficiently spliced because of suboptimal signals at the 3′ splice site. J. Virol. **68:**3071–3079.
56. **Sterner, D. A., and E. C. Murphy.** 1992. Regulation of the efficiency and thermodependence of murine sarcoma virus MuSVts110 by sequences in both exons. Virology **191:**638–648.
57. **Stoltzfus, C. M.** 1989. Synthesis and processing of avian sarcoma retrovirus RNA. Adv. Virus Res. **35:**1–38.
58. **Stoltzfus, C. M., and S. J. Fogarty.** 1989. Multiple regions in the Rous sarcoma virus *src* intron act in *cis* to affect the accumulation of unspliced RNA. J. Virol. **63:**1669–1676.
59. **Sun, J.-S., and J. L. Manley.** 1995. A novel U2-U6 snRNA structure is necessary for mammalian mRNA splicing. Genes Dev. **9:**843–854.
60. **Tarn, W. Y., and J. A. Steitz.** 1994. SR proteins can compensate for the loss of U1 snRNP functions *in vitro*. Genes Dev. **8:**2704–2717.
61. **Tazi, J., C. Alibert, J. Temsamani, I. Reveillaud, G. Cathala, C. Brunel, and P. Jeanteur.** 1986. A protein that specifically recognizes the 3′ splice site of mammalian introns is associated with a small nuclear ribonucleoprotein. Cell **47:**755–766.
62. **Wassarman, D. A., and J. A. Steitz.** 1992. Interactions of small nuclear RNAs with precursor messenger RNAs during *in vitro* splicing. Nature (London) **349:**463–464.
63. **Wu, J., and J. Manley.** 1989. Mammalian pre-mRNA branch site selection by U2 snRNP involves base pairing. Genes Dev. **3:**1553–1561.
64. **Wyatt, J. R., E. J. Sontheimer, and J. A. Steitz.** 1992. Site-specific crosslinking of mammalian U5 snRNP to the 5′ splice site before the first step of splicing. Genes Dev. **6:**2542–2553.
65. **Zahler, A. M., and M. B. Roth.** 1995. Distinct functions of SR proteins in recruitment of U1 small nuclear ribonucleoprotein to alternative 5′ splice sites. Proc. Natl. Acad. Sci. USA **92:**2642–2646.
66. **Zamore, P. D., J. G. Patton, and M. R. Green.** 1992. Cloning and domain structure of the mammalian splicing factor U2AF. Nature (London) **355:**609–614.
67. **Zhang, L., and C. M. Stoltzfus.** 1995. A suboptimal 3′ splice site is necessary for efficient replication of Rous sarcoma virus. Virology **206:**1099–1107.
68. **Zhuang, Y., A. M. Goldstein, and A. M. Weiner.** 1989. UACUAAC is the preferred branch site for mammalian mRNA splicing. Proc. Natl. Acad. Sci. USA **86:**2752–2756.
69. **Zhuang, Y., and A. M. Weiner.** 1989. A compensatory base change in human U2 snRNA can suppress a branch site mutation. Genes Dev. **3:**1545–1552.